

# Numerical solution of nonlinear electron kinetic equation in self-similar variables

I. F. POTAPENKO<sup>1</sup> and S. I. KRASHENINNIKOV<sup>2</sup>

<sup>1</sup>Keldysh Institute of Applied Mathematics, RAS, 125047 Moscow, Russian Federation  
(firena@yandex.ru, irina@keldysh.ru)

<sup>2</sup>University of California at San Diego, La Jolla, San Diego, CA 92093, USA

(Received 13 April 2011, revised 22 April 2011 and accepted 7 May 2011;  
first published online 9 June 2011)

**Abstract.** We present numerical solution of a fully nonlinear electron kinetic equation in self-similar variables, which on the one hand has all features of a ‘standard’ hydrodynamics (ratios of the electron mean free path to the scale length  $\gamma \equiv \lambda_C/L \ll 1$ ), and on the other hand has no restriction on the smallness of the parameter  $\gamma$ . The self-similar variable approach reduces dimensionality of the space-dependent kinetic equation, thereby providing numerical analysis of the electron heat transport in the velocity space. The electron distribution structure and its super thermal power-law tail are examined.

PACS number(s): 52.25.Dg, 52.65.Ff, 52.50.-b

---

## 1. Introduction and statement of the problem

The paper is organized as follows. The first section contains introduction, preliminary discussion and statement of the problem. In Section 2, we consider an equation that is computed at first examining the separate influence of its constituent operators and shortly discussing numerical issues. The illustrative simulation results are presented graphically. Concluding remarks follow at the end.

Kinetic treatment of plasma systems plays an important role in a description of macroscopic plasma properties that cannot be learned under hydrodynamic approach. The Boltzmann kinetic equation (BKE) is a cornerstone for the study of transport phenomena in gases and plasmas, as well as the photon, neutron, phonon etc. transport in different media [1–6].

For the one-dimensional in space electron distribution function  $f(x, v, t)$  BKE reads

$$\frac{\partial f}{\partial t} + v_x \frac{\partial f}{\partial x} - \frac{eE(x)}{m} \frac{\partial f}{\partial v_x} = C_e(f), \quad (1.1)$$

where  $e$  and  $m$  are the electron charge and mass, respectively, and  $E(x)$  is an external electrical field as it is usually assumed dealing with transport processes. The operator  $C_e(f) = C_{ee}(f, f) + C_{ei}(f)$  describes electron–electron and electron–ion collisions. For spatially uniform problem  $\partial f / \partial x = 0$ , the kinetic equation is of the Landau–Fokker–Planck (LFP) type. The nonlinear electron–electron collisional integral  $C_{ee}(f, f)$  in

the Landau form reads

$$\left(\frac{2\pi e^4 A n}{m^2}\right)^{-1} C_{ee}(f, f) = \frac{\partial}{\partial v_i} \left\{ \int dw U_{ij} \left( \frac{\partial}{\partial v_j} - \frac{\partial}{\partial w_j} \right) f(v)f(w) \right\}, \quad (1.2)$$

$$U_{ij} = \frac{u^2 \delta_{ij} - u_i u_j}{u^3}, \quad |u| = |v - w|,$$

where  $A$  is the Coulomb logarithm and  $n$  is the electron density.

Direct solving of the BKE is a rather complicated problem for several reasons, therefore the most common approach to transport problems in gases and plasmas is based on successive expansion of the distribution function  $f(x, v, t)$  in the Taylor series over small parameter  $\gamma$ , with further derivation of ‘hydrodynamic’ equations for some moments of the locally equilibrium distribution function, by taking into account only first-order corrections over small parameter  $\gamma$ . These small parameters assume rather long scales of spatiotemporal evolution of the media in comparison to both particle mean free path  $\lambda_C \ll L$  and time between particle collisions  $t_e \ll t$ . Here  $\lambda_C = T^2/2\pi e^4 A n$ ,  $t_e = m^2 v_{th}^{3/2}/2\pi e^4 A n$  and  $v_{th} = (2T/m)^{1/2}$  is the thermal velocity.

However, generally speaking it is not clear *a priori*, how small  $\gamma$  should be to insure reasonable accuracy of hydrodynamic transport equations. For example, in order to use the Spitzer–Harm expression for electron heat conduction [7] with reasonable accuracy,  $\gamma$  should be below just few  $\times 10^{-2}$  (e.g. see Ref. [8]). The reason for this is a strong increase of the Coulomb mean free path,  $\lambda_C$ , with electron energy,  $\varepsilon$  ( $\lambda_C \sim \varepsilon^2$ ), so that electrons responsible for heat transport ( $\varepsilon \sim 10 \times T$ , where  $T$  is the electron temperature) are much less collisional than for thermal ones.

Meanwhile  $\gamma \sim 0.1$  are often observed in many applications (e.g. in edge plasma of fusion devices, ICF studies, space plasmas etc.), which shows the needs for the models going beyond a ‘standard’ hydrodynamics. Extension of the ‘standard’ hydrodynamic equations by taking into account higher order terms over parameter  $\gamma$  does not look very attractive because of possible impact of non-expandable terms (e.g.  $\exp(-1/\gamma^p)$ , where  $p$  is some constant) existing in the solution of the BKE (see below).

In order to overcome the problem arising from the solution of the BKE by the Taylor expansion of the distribution function, other methods of approximate solution of the BKE were suggested for both plasma and neutral gas (e.g. see Ref. [8–11] and the references therein). However, it is difficult to judge on both accuracy and applicability limits of these approaches related to kinetic description without some exact reference solutions of the BKE.

One of the issues with the solution of even stationary BKE is its high dimensionality, at least 1D2V, see (1.1). However, in Ref. [12] it was shown that for some cases the electron BKE allows exact representation in self-similar variables that resulted in reducing dimensionality, which makes the equation more tractable. Dealing with the kinetic equation, the velocity and particle distribution are usually normalized to  $v_{th}$  and  $n \cdot v_{th}^{-3}$ . In Ref. [12] it was suggested to represent the one-dimensional in space azimuthally symmetric electron distribution function  $f(x, v, t)$  as a product of  $\tilde{f}(\tilde{v}, \mu, t) \cdot T(x)^{-\alpha} \cdot N$ , where  $T(x)$  is the effective electron temperature,  $\tilde{v} = v/v_{th}$ ,  $\alpha$  is an adjustable parameter,  $\mu = \cos(\vartheta)$  and  $\vartheta$  is the azimuthal angle,  $N$  is the normalization constant and  $n(x) \propto [T(x)]^{3/2-\alpha}$ . Such solutions are possible for specific profiles, which make parameter  $\gamma$  independent of space  $x$ . Namely, effective

temperature  $T(x)$  satisfies equation  $T^{\alpha-1/2} \cdot \frac{dT}{dx} = \text{const}$ , then

$$\gamma = -\frac{T^2}{2\pi e^4 A n} \cdot \frac{d \ln T}{dx} = \text{const}.$$

For such profiles, density and temperature profile the stationary,  $\partial f / \partial t = 0$  electron kinetic equation (1.1) with  $C_{ei}(f)$  describing electron-ion angle scattering only, then

$$\frac{m^2}{2\pi e^4 A n(x)} C_{ei}(f) = \frac{Z}{v^3} \left\{ \frac{\partial}{\partial \mu} [(1 - \mu^2) v f] \right\}$$

can be transformed into

$$\gamma \mu v \left( \alpha f + v/2 \frac{\partial f}{\partial v} \right) - \frac{\gamma E}{2} \left[ \mu \frac{\partial f}{\partial v} + \frac{1}{v} (1 - \mu^2) \frac{\partial f}{\partial \mu} \right] = \frac{1}{4} [C_{ee}(f, f) + C_{ei}(f)]. \quad (1.3)$$

Omitting tilde sign we returned to the original notations. The normalized ambipolar electron field  $\gamma_E = \frac{E}{E_D} = \frac{e E T}{2\pi e^4 L n}$  equalizes flux current to zero;  $Z$  is an effective ion charge. In Ref. [12] (1.3) was solved analytically for small  $\gamma$  and  $Z = 1$  by choosing appropriate domains of variable  $v$  with further analytic continuations of function  $f$  allowing to match the solutions in different domains. Similar approach has been used before for the solution of the problem of runaway electrons in DC electric field [13–15]. In Ref. [12] it was found that function  $f$  has a power-law tail

$$f(v, \mu)_{v^2 \gg \gamma^{-1/2}} \propto \exp \left( -\frac{2}{3} \gamma^{-1/2} - \frac{(2\pi)^{3/2}}{\Gamma(1/4)^2} \gamma^{-1/4} \right) \frac{\Phi(\mu)}{v^{2x}}. \quad (1.4)$$

As one sees, the magnitude of this tail has non-expandable terms that cannot be recovered by the Taylor expansion.

In Ref. [16] the analytic solution for (1.3) was extended to the case of high  $Z$ . We note that the solutions for high  $Z$ , having no power-law tail, found in Ref. [17] are erroneous, as they are found assuming that the term containing electric field is a dominant one, while simple examination of (1.3) shows that the first ballistic term always dominates, what can be also seen further from numerical simulation. In Ref. [18], self-similar variables were used to analyze neutral transport governed by charge-exchange processes in edge plasma.

Even though analytic solutions of (1.3) provide some useful information on the electron distribution function (e.g. the magnitude and the form of the tail), it is difficult to use them for benchmarking the models targeting quantitative evaluation of heat flux for the case going beyond the Spitzer–Harm approximation. Therefore, in Ref. [19] (1.3) was solved numerically for the linear kinetic equation, adopting the Rosenbluth potentials for the Maxwellian distribution function (FP form of the equation). Although the power-law tail in these numerical solutions, in agreement with Ref. [12], was recovered, they are lacking agreement with the Spitzer–Harm limit where the Rosenbluth potentials should be found self-consistently, *i.e.* nonlinear kinetic equation should be considered.

In what follows we present for the first time numerical solution of the nonlinear electron kinetic equation in self-similar variables, which on the one hand has all features of a ‘standard’ hydrodynamics (e.g. Spitzer–Harm limit of electron heat conduction, very small  $\gamma$ ), and on the other hand has no restriction on the smallness of parameter  $\gamma$ . In the next section we present numerical simulation results.

## 2. Solution of the time-dependent kinetic equation

Strictly speaking one cannot state the existence of solution to (1.3) for several reasons. A complexity of the equation makes possible its analytical treatment under simplifying assumptions, thus providing us with asymptotic solutions. In order to find the solutions for (1.3) numerically, the relaxation method is used, *i.e.* instead of stationary (1.3) the time-dependent equation

$$\partial f / \partial t + \Gamma f + E f = [C_{ee}(f, f) + C_{ei}(f)] / 4 \quad (2.1)$$

is employed for computing the electron distribution function evolution, where  $\Gamma f$  and  $E f$  are the ballistic and electrical field operators, respectively, from (1.3). The electron distribution is normalized to unity, *i.e.*  $n = \int_0^\infty dv v^2 \int_{-1}^1 d\mu f(v, \mu, t) = 1$  and  $\varepsilon = \int_0^\infty dv v^4 \int_{-1}^1 d\mu f(v, \mu, t) = 1$ , where  $n$  and  $\varepsilon$  correspond to the electron density and energy, respectively. As usual, the distribution function (or its derivatives) is bounded at  $v = 0$ ,  $\mu = \pm 1$  and tends to be zero  $f \rightarrow 0$  with  $v \rightarrow \infty$  fast enough ensuring the moment  $\varepsilon$  is limited. The local Maxwell distribution corresponding to the time-dependent thermal velocity defined as  $v_{th} = \sqrt{2\varepsilon/3} \simeq v_{th}(0)$  is  $f_{Maxw}(v, t) = 2\pi^{-1/2} v_{th}^{-3} \cdot \exp(-v^2/v_{th}^2)$ . For simplicity, the initial condition on the distribution function  $f(v, \mu, 0) = f_0(v)$  is set to the Maxwell distribution. The evolution of the distribution tails in high velocity region  $v \gg v_{th}$  for  $t \gg t_e$  and formation of the non-equilibrium steady-state electron function is searched. Before we proceed with presentation of numerical results it would be helpful to analyze constituent operators contained in (1.3) and (2.1) and roughly estimate the solution we are going to obtain for different input parameters. Dealing with the numerical solution it is practicable to have firm references to compare with. The Maxwell distribution and asymptotic solution (1.4) play an important role particularly for the verification of numerical results.

It is well known that the collisional integral action can be formally subdivided into a Coulomb diffusion part and a transport term. The influence of Coulomb diffusion is the utmost in the cold energetic region  $0 \leq v < v_{th}$ , where the solution acquires a quasi equilibrium form within the period of collision time  $t_e$ . The time period when the relaxation of the distribution bulk is finished is characterized for our normalization in (2.1) by  $t_e \sim 4$ . In high velocity region,  $v \gg v_{th}$ , the LFP nonlinear parabolic equation degenerates because of the known Rutherford cross-section dependence on velocity and the transport term (the first derivative) becomes more important. This condition leads to inevitable retarding of the distribution tail formation in comparison to the bulk part of the distribution (at least,  $t > 20$  in numerical simulation). Operator  $C_{ei}(f)$  contributes to the electron distribution function isotropization. Big magnitude of charge  $Z$  leads to the faster Maxwellization of the distribution and mainly in the thermal velocity region.

Integrating over velocity space both sides of (2.1) with corresponding weights, we obtain the following laws for changing of distribution function moments with time

$$\begin{aligned} \frac{dn}{dt} &= \gamma(\alpha - 2)J; & \frac{dJ}{dt} &= \gamma(\alpha - 5/2)\varepsilon_{\parallel} - \frac{\gamma E}{2}n, \\ \frac{d\varepsilon}{dt} &= \gamma(\alpha - 3) \int_0^\infty dv v^5 \int_{-1}^1 d\mu \mu f(v, \mu, t) - \gamma E J, \end{aligned} \quad (2.2)$$

where parallel component of energy is denoted as  $\varepsilon_{\parallel} = \int_0^{\infty} dv v^4 \int_{-1}^1 d\mu \mu^2 f(v, \mu, t)$ . It has been mentioned above that the problem presumes to be a no-current condition, thus  $J = \int_0^{\infty} dv v^2 \int_{-1}^1 d\mu v \mu \cdot f(v, \mu, t) = 0$  has to be fulfilled by suitably chosen value of ambipolar field  $\gamma_E$ . As can be seen from (2.2), if  $J \approx 0$ , then during the whole process under consideration the electron density  $n$  remains constant. The energy  $\varepsilon(t)$  slightly increases in time proportionally to the fifth moment (density energy flux) multiplied by factor  $\gamma(\alpha - 3)$ . Our goal is to preserve the macroscopic laws (2.1) in discrete case by adequate approximation in numerical schemes. For the LFP nonlinear kinetic equation the completely conservative implicit finite-difference scheme is used with iterations over nonlinearity (e.g. see Ref. [20] and the references therein). The well-known specific property of the kinetic equation is that the form of the operators that is taken for discrete approximation is of great importance. For operator  $Ef$  this is the well-known form of the density conservation (differential) law (e.g. see Ref. [21, 22] and references therein)

$$Ef = \frac{\gamma_E}{2} \frac{1}{v^2} \left\{ \frac{\partial}{\partial v} (\mu v^2 f) + \frac{\partial}{\partial \mu} [(1 - \mu^2) v f] \right\}. \tag{2.3}$$

The action of this operator leads to the well-known runaway effect when the distribution stretching is moved in the field direction  $\mu = 1$  toward the high velocity region  $v > v_{cr} \approx \gamma_E^{-1}$  except for the quasi isotropic part in the cold velocity region because of collisions. Current  $dJ/dt \sim \gamma_E n$  resulted from the strong splitting of the distribution function over all ‘directions’  $\mu$  grows in time as well as in energy. But the temperature of tail particles remains less than the temperature of thermal particles (the local Maxwellian distribution). The value of energy growth  $d\varepsilon/dt \sim \gamma_E J$  is connected in our case with the parameter  $\gamma(\alpha - 3)$ .

Further, we consider equation  $\partial f / \partial t + \Gamma f = 0, f(v, \mu, 0) = f_0(v, \mu)$  with the ballistic operator  $\Gamma f$  that can be written in different forms, for example

$$\Gamma f = \gamma \mu v \left( \alpha f + \frac{v}{2} \frac{\partial f}{\partial v} \right) = \frac{\gamma}{2} \frac{1}{v^3} \frac{\partial}{\partial v} (\mu v^5 f) + \gamma \mu \left( \alpha - \frac{5}{2} \right) v f = \gamma \mu \frac{1}{v^{2\alpha-2}} \frac{\partial}{\partial v} (v^{2\alpha} f).$$

The last form gives an idea about the character of a solution

$$f(v, \mu, t) = f_0 \left( \frac{v}{1 + v \mu \gamma t / 2} \right) \left( \frac{1}{1 + v \mu \gamma t / 2} \right)^{2\alpha}. \tag{2.4}$$

The following representation for  $\Gamma f$  is used in numerical simulation

$$\Gamma f = \frac{\gamma}{2} \frac{1}{v^2} \frac{\partial}{\partial v} (\mu v^4 f) + \gamma \mu (\alpha - 2) v f.$$

This form yields the correct approximation of the law  $dn/dt$  in (2.1) that can be naturally obtained in discrete case. Note that at the beginning the value of  $\gamma_E$  may be estimated from equality  $\gamma_E \approx 2/3 \gamma (\alpha - 2.5)$  in (2.2). Thereby in the course of computing, at every time step two iterative loops are carried out. Firstly, iterations on  $\gamma_E$  are made until  $J \approx 0$ , and secondly, iterations are developed over nonlinearity until the numerical solution converges with preset accuracy. The effect of operators (2.3) and (2.4) upon initial function should become apparent approximately within a while  $t \approx \gamma_E^{-1}, (\alpha \gamma)^{-1}$ .

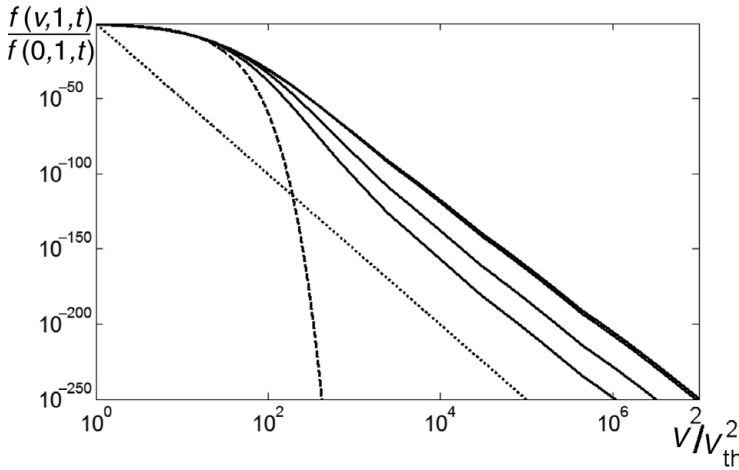
Operator (2.1) is solved in full formulation (full velocity space) avoiding any additional restrictions (artificial cutoff of the distribution at the rated interval).

Specifically, the boundary condition  $\lim_{v \rightarrow \infty} f = 0$  in the discrete case means that the numerical distribution function has to be equal to machine zero at the maximum mesh speed  $f(v_{\max}, \mu, t) = 0$ . This condition has to be satisfied properly for taking into account high energetic distribution tails and preserving the conservation laws (for numerical aspects concerning the LFP equation, see, for example [20] and the references therein).

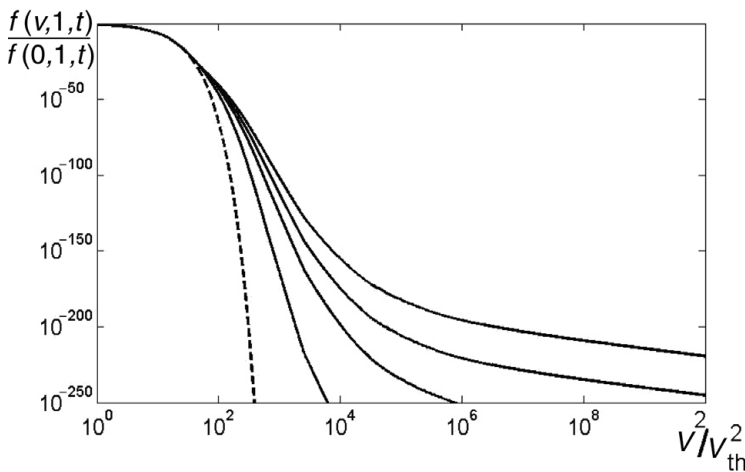
Further simulation results of (2.1) are illustrated on pictures 1–5 for different parameters  $\alpha$ ,  $\gamma$ ,  $\gamma_E$ . For all cases,  $J \approx 0, n \approx 1$  are preserved with the approximation error less than  $10^{-8}$ . Big value of  $\alpha$  defines the lower electron function tails and their steeper slope, see (2.4). Correspondingly, it defines big value of  $\gamma_E$  and slight energy increase. In considered cases the energy growth does not exceed 5% of initial value. Parameter  $\gamma$  mainly determines the time of the distribution function developing. Illustrative examples prove all that has been stated above. In the region  $v \leq v_{\text{th}}$  the distribution functions are close to the Maxwellian (dashed line) and close to each other throughout the entire relaxation. Temporal evolution of the electron distribution function in the direction  $\mu = 1$  is presented in logarithmic scale versus logarithm of squared velocity. In all pictures distribution functions are normalized on their value at  $v = 0$ . Also, the plots of the distribution are given for  $\mu = -1, 0, 1$  at the moment when power-law tails are already formed.

Figure 1 demonstrates the steady-state non-equilibrium distribution formation at the time moments,  $t = 5, 10, 25, 50$  for parameters  $\alpha = 50$  and  $\gamma = 0.005$ . It is seen that solution is established up to the moment  $t = 25$ . In agreement with the analytic result (1.4), the function has power-law tail (dotted line denotes  $v^{-2\alpha}$ ). Figure 2 shows temporal evolution of  $f(v, \mu = 1, t)$  for  $\alpha = 5$  and  $\gamma = 0.0002$ . At time moment  $t = 350$  the tail (1.4) is already developed. Figure 3 shows the distribution function  $f$  at  $\mu = -1, 0, 1$  and  $t = 75$  for the same parameter  $\alpha = 5$  but five times bigger  $\gamma = 0.001$ . As can be seen from comparison of Figs. 2 and 3 the value of  $\gamma$  mainly defines the time period of the distribution tail formation. Finally two plots of the distribution function, Figs. 4 and 5, are shown for  $\alpha = 100$  and  $\gamma = 0.001$  (for these parameters  $\gamma_E \approx 0.06$ ). Figure 4 demonstrates the temporal evolution of the electron function with the distribution profiles falling more steeply in agreement with (1.4) and (2.4). Energy is rising up to  $\varepsilon(t) \approx 1.05 \cdot \varepsilon(0)$  during the considered time period and superthermal distribution tail is constantly developing because of changing  $v_{\text{th}}(t)$ . Figure 5 shows the distribution in a colder part of velocity in more detail for  $\mu = -1, 0, 1$  at  $t = 200$ . Computed function coincides with the Maxwell distribution (dashed line) in the velocity region up to  $v^2 \leq (3v_{\text{th}})^2$ . In agreement with formula (2.4), the distribution function is disintegrated over direction  $\mu$  because of the ballistic operator action. From the numerical results for different input parameters it can be concluded that the ballistic term has always prevailed.

We notice that speculations extensively discussed in literature in connection to the generalization of the Boltzmann–Gibbs statistics are chiefly addressed to recipe for generating significant high-energy tails, mostly in space plasmas (e.g. [23] and references therein). The issues with runaway and power law tails are not limited to the Coulomb collisions of electrons but possible for environments with different electron scattering laws. For example, runaway of electrons in external electric field was considered in Ref. [24] when only electron-neutral interactions matter. In Ref. [25] it was shown that peculiar dependence of resistivity on electric field in



**Figure 1.** Temporal evolution of electron distribution function for  $\mu=1$  normalized on its value at zero velocity versus squared velocity is shown in double logarithmic scale (arbitrary units);  $\alpha=50$ ,  $\gamma = 0.005$ ,  $t = 5, 10, 25, 50$ . Dashed line is the Maxwellian distribution and dotted line is  $v^{-2\alpha}$ .



**Figure 2.** Temporal evolution of the electron distribution function for  $\alpha=5$ ,  $\gamma=0.0002$  and  $t=200, 300, 350, 400$ .

n-InSb and n-GaAs at the temperatures 1–10 K could be explained by power-law tail of the electron distribution function. In Ref. [26] the runaway was studied in a weakly ionized gas subjected to a weak electric field. The qualitative behavior of the time-dependent electron distribution for different velocity dependence of collision frequency  $\nu \sim v^{-n}$  (that corresponds to the long-range interaction  $U \propto r^{-s}$  and impenetrable elastic spheres) was examined. Subsequently elaborated methods were applied for solid-state plasmas to examine the development of the electron velocity distribution in n-InSb at helium and hydrogen temperatures. It might be also worth to mention Refs. [27, 28] where the evolution of the velocity distribution tails for systems with long-range interaction governed by the LFP equation were studied.

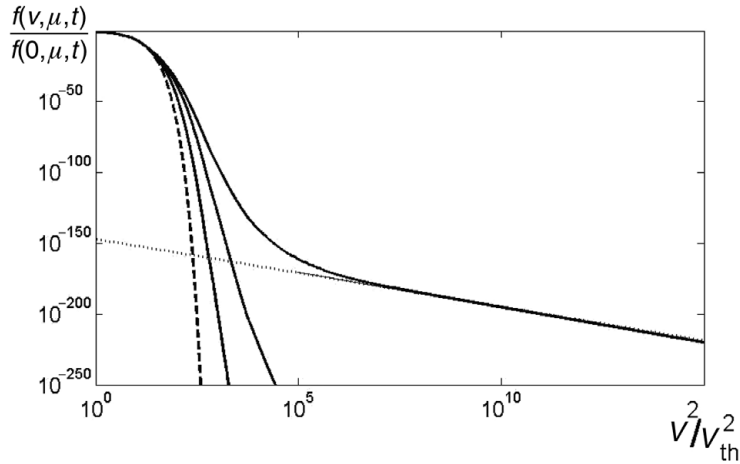


**Figure 3.** Electron distribution function for  $\mu = -1, 0, 1$  and  $\alpha = 5$ ,  $\gamma = 0.001$ ,  $t = 75$ . Dashed line is the Maxwellian distribution and dotted line is  $v^{-2\alpha}$ .

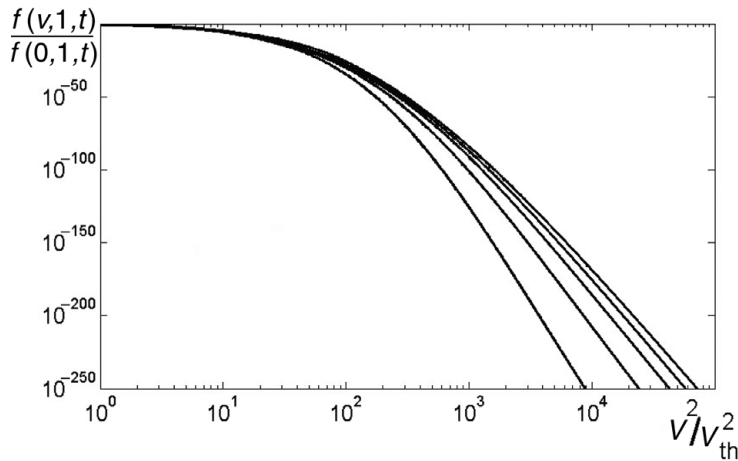


**Figure 4.** Temporal evolution of electron distribution function for  $\alpha = 100$ ,  $\gamma = 0.001$  and  $t = 25, 50, 75, 100, 150$ .

Accelerated high-energy distribution tails are observed in lab plasma, particularly in the tokamak scrape-off layer, in space and solid-state plasmas and their behavior attract increasing interest.

### 3. Conclusions

We present numerical solution of a nonlinear electron kinetic equation in self-similar variables, which on the one hand has all features of a ‘standard’ hydrodynamics (ratios of the electron mean free path to the scale length  $\gamma \equiv \lambda_c / L \ll 1$ ), and on the other hand has no restriction on the smallness of parameter  $\gamma$ . The self-similar variables approach developed previously reduces dimensionality of the



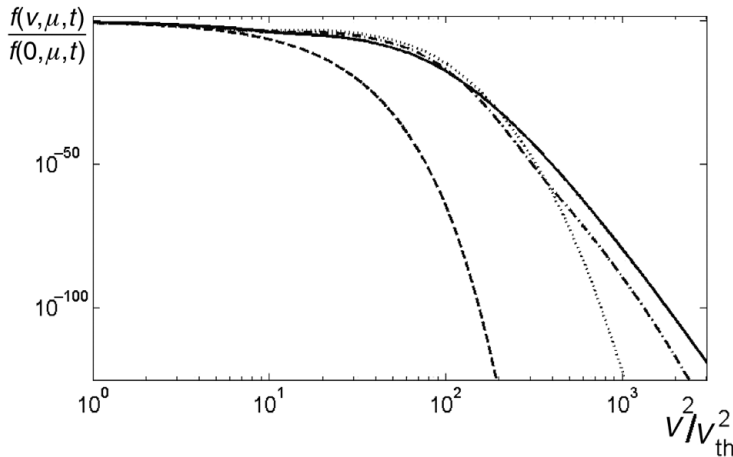


**Figure 5.** Electron distribution function for  $\alpha = 100$ ,  $\gamma = 0.001$ ,  $t = 200$ ;  $\mu = -1$  dotted line,  $\mu = 0$  – dashed-dot line,  $\mu = 1$  – solid line. Dashed line is the Maxwellian distribution.

space-dependent kinetic equation and makes available numerical analysis of the electron heat transport only in the velocity space. Validation and verification of the exploited numerical schemes are proved. The problem is unfolded through a time-dependent numerical solution that tends to the non-equilibrium stable electron distribution. Structure of the electron distribution function is analyzed in detail, and asymptotic results are confirmed. Self-similar numerical solutions of the electron kinetic equation are available and can be used for benchmarking both reduced models and codes for laboratory, space and solid-state plasmas.

## Acknowledgments

This work is supported in part by the Program of Presidium of Russian Academy of Sciences 14 (3.1).

## References

- [1] Chapman, S. and Cowling, T. 1970 *Mathematical Theory of Non-uniform Gases*. Cambridge, UK: Cambridge University Press.
- [2] Grad, H. 1949 *Commun. Pure and Appl. Math.* **2**, 331.
- [3] Cercignani, C. 1975 *Theory and Application of the Boltzmann Equation*. Edinburgh, UK: Scottish Academic Press.
- [4] Braginskii, S. I. 1965 Transport processes in a plasma. In: *Review of Plasma Physics*, Vol. 1. New York: Consultants Bureau.
- [5] Landau, L. D. and Lifshitz, E. M. 2002 *Course of Theoretical Physics*, Vol 10: “Physical Kinetics” (ed. L. P. Pitaevskii and E. M. Lifshitz). Oxfordshire, UK: Pergamon Press.
- [6] Chandrasekhar, S. 1960 *Radiative Transfer*. New York: Dover.
- [7] Spitzer, L. and Harm, R. 1953 *Rev. Phys.* **89**, 977.
- [8] Luciani, J. F., Mom, P. and Virmont, J. 1983 *Phys. Rev. Lett.* **51**, 1664.
- [9] Albritton, J. R., Williams, E. A., Bernstein, I. B. and Swartz, K. P. 1986 *Phys. Rev. Lett.* **57**, 1887.

- [10] Krasheninnikov, S. I. 1993 *Phys. Fluids B* **5**, 74.
- [11] Belyi, V. V., Demaulin, W. and Paiva-Veretennikoff, I. 1989 *Phys. Fluids B* **1**, 305, 317.
- [12] Krasheninnikov, S. I. 1988 *Sov. Phys. JETP* **67**, 2483.
- [13] Gurevich, A. V. 1961 *Sov. Phys. JETP* **12**, 904.
- [14] Lebedev, A. N. 1965 *Zh. Exp. Teor. Fiz.* **48**, 1396.
- [15] Connor, J. W. and Hastie, R. J. 1975 *Nucl. Fusion* **15**, 415.
- [16] Krasheninnikov, S. I. and Bakunin, O. G. 1992 *Contrib. Plasma Phys.* **32**, 255; Bakunin, O. G. and Krasheninnikov, S. I. 1995 *Plasma Phys. Reports* **21**, 502.
- [17] Batishchev, O. V., Bychenkov, V. Yu., Detering, F., Rozmus, W., Sydora, R., Capjack, C. E. and Novikov, V. N. 2002 *Phys. Plasmas* **9**, 2302.
- [18] Helander, P. and Krasheninnikov, S. I. 1996 *Phys. Plasmas* **3**, 226.
- [19] Krasheninnikov, S. I., Dvornikova, N. A. and Smirnov, A. P. 1990 *Contrib. Plasma Phys.* **30**, 67.
- [20] Potapenko, I. F., Bobylev, A. V. and Mossberg, E. 2008 *Transp. Theory Stat. Phys.* **37**, 113.
- [21] Killeen, J., Kerbel, G. D., McCoy, M. G. and Mirin, A. A. 1986 *Computational Methods for Kinetic Models of Magnetically Confined Plasmas*. New York: Springer-Verlag.
- [22] Dnestrovskij, Yu. N. and Kostomarov, D. P. 1986 *Numerical Simulations of Plasmas*. Berlin, Germany: Springer-Verlag.
- [23] Meyer-Vernet, N. 2001 *Planet. Space Sci.* **49**, 247.
- [24] Gurevich, A. V., Millikh, G. M. and Roussel-Dupre, R. 1992 *Phys. Lett. A* **165**, 463.
- [25] Levinson, I. B. 1965 *Sov. Phys. – Solid State* **6**, 1952.
- [26] Stenflo, L. 1966 *Plasma Phys.* **8**, 665.
- [27] Potapenko, I. F., Bobylev, A. V., Azevedo, C. A., Assis, A. S. 1997 *Phys. Rev. E* **56**, 7159.
- [28] Chavanis, P-H. and Lemou, M. 2005 *Phys. Rev. E* **72**, 061106.